Waveguide-based single-shot temporal cross-correlator

2015 J. Opt. 17 035501

(http://iopscience.iop.org/2040-8986/17/3/035501)

IOP Publishing Journal of Optics
J. Opt. 17 (2015) 035501 (5pp) doi:10.1088/2040-8978/17/3/035501

Waveguide-based single-shot temporal cross-correlator

Moti Fridman[1], Yoshitomo Okawachi[2], Stéphane Clemmen[2], Michaël Ménard[2], Michal Lipson[2] and Alexander L Gaeta[2]

[1] Faculty of Engineering, Bar Ilan University, Ramat Gan 52900, Israel
[2] School of Applied and Engineering Physics, Cornell University, Ithaca, NY 14853, USA

E-mail: mordechai.fridman@biu.ac.il

Received 24 November 2014, revised 21 December 2014
Accepted for publication 30 December 2014
Published 2 February 2015

Abstract

We describe a novel technique for performing a single-shot optical cross-correlation in nanowaveguides. Our scheme is based on four-wave mixing (FWM) between two orthogonally polarized input signals propagating with different velocities due to polarization mode dispersion. The cross-correlation is determined by measuring the spectrum of the idler wave generated by the FWM process.

Keywords: correlators, nonlinear optical signal processing, waveguides

(Some figures may appear in colour only in the online journal)

1. Introduction

Cross-correlation gives a measure for the similarity between two input signals, therefore, it is implemented in numerous data processing systems [1–13]. Today, the calculation of the cross-correlation is done in an electronic processing unit [14] and since most of the data communication is transferred via optical fibers, an optics-to-electronics convertor is needed. This convertor is slow compared to the flow of information in the optical fibers and imposes an electronic bottleneck on optical communication systems. Optical routers can eliminate the bottleneck and a key element in optical routers is the optical cross-correlation device for header detection [1, 2]. Optical cross-correlation is needed for pattern recognition in triggering ultrafast cameras [3, 4]. Both optical routers and ultrafast camera triggers require cross-correlation of non-repetitive signals and in both cases the cross-correlator should be embedded in a fiber or a waveguide. Optical cross-correlation is also a commonly used technique for ultrashort pulse characterization [5, 6] and with the rise of ultrashort fiber lasers, it is important to develop a technique for analyzing a single-shot pulse in a waveguide. Many approaches for optical cross-correlation have been developed, including mechanically moving filters [7], diffraction in free space [8, 10] and nonlinear based approaches [9, 10]. However, all these techniques are slow, performed in free space or require repetitive signals.

Here we present, an ultrafast optical cross-correlator that utilizes the nonlinearity and polarization mode dispersion (PMD) of a nanowaveguide to perform a single-shot cross-correlation. We note that the PMD rises from the birefringence of the waveguide which is engineered by manipulating the cross-section of the waveguide. We show that the spectrum of the idler wave generated from the interaction of two orthogonally-polarized chirped input waves (signal and pump) via four-wave mixing (FWM) yields the cross-correlation of the two inputs. Our system is similar to a XFROG configuration [11–13], however, it is fully integrated inside waveguides which is more suitable for ultrafast fiber lasers, increases robustness, efficiency and reduces the cost.

2. Theoretical background

Our technique for performing the cross-correlation is based on the FWM process within a waveguide between the pump and the signal waves with amplitudes A_p and A_s, respectively. This interaction yields an idler wave with an amplitude $A_i(t)$,

given by

$$A_i(t) \propto A_s(t)^* A_p^2(t). \tag{1}$$

Integrating over time to obtain the measured intensity I_i by slow detectors, yields

$$I_i = \int A_i^2(t)\mathrm{d}t \propto \int \left(A_s(t)^* A_p^2(t)\right)^2 \mathrm{d}t. \tag{2}$$

Thus, the measured amplitude of the idler wave, which is equal to square root of I_i, is proportional to the correlation between the signal wave and the square of the pump wave. To find the correlation between an input signal and a temporal filter, the pump wave needs to be tailored as square root of the desired filter. The resulting amplitude of the idler wave equals to the correlation between the input signal and the filter.

A measurement of cross-correlation requires the input signal to pass through the other input signal while measuring the correlation between them at each time. This is accomplished by rotating the polarization of the pump wave with respect to the signal wave such that the polarizations of the two beams are orthogonal to each other. In the presence of PMD in the waveguide, the signal wave and the pump wave travel with different group velocities due to birefringence so one passes through the other.

We inject the signal ahead of the pump wave with an initial temporal separation Δt. As the two waves propagate through the waveguide, the pump passes through the signal wave so Δt changes. Due to FWM interaction between the pump and the signal waves an idler wave is generated at each Δt. The idler amplitude as a function of time is proportional to the correlation as a function of Δt. To obtain the cross correlation, we need to measure the idler intensity as a function of time [15, 16], however, this is not possible for an ultrashort signal wave with fluctuations of less than a picosecond. To obtain these ultrafast fluctuations, we map time-to-frequency by suitably chirping the signal and the pump waves in such a way that the frequency of the idler wave is a function of the temporal delay, Δt. Thus, for different temporal separations the generated idler wave has different frequency.

We illustrate this concept by assuming that the frequency of the chirped signal wave as a function of time expressed as

$$\omega_s(t) = \omega_{s0} + \alpha(t + \Delta t), \tag{3}$$

where ω_{s0} is the central frequency of the signal wave, and α is the slope of the chirping. Since the frequency of the resulting idler is

$$\omega_i = 2\omega_p - \omega_s, \tag{4}$$

the appropriate slope of the chirped pump should be $\alpha/2$ such that

$$\omega_p(t) = \omega_{p0} + \frac{\alpha}{2}t, \tag{5}$$

where ω_{p0} is the central frequency of the pump wave. The frequency of the generated idler is then

$$\omega_i(t) = 2\omega_{p0} - \omega_{s0} - \alpha\Delta t. \tag{6}$$

It can be seen from equations (2)–(4) that although the signal and the pump waves are chirped (their frequencies depend linearly on t), the idler wave is not chirped. Namely, the frequency of the idler wave is constant in time and depends only on the temporal separation between the signal and the pump waves. The bandwidth of the idler wave is proportional to the instantaneous bandwidth of the idler and signal waves which depended on the chirping and on the FWM time scale. For a temporal separation Δt between the signal and the pump waves, equation (1) yields

$$A_i(\Delta t) \propto \int A_s(\tau + \Delta t) A_p^2(\tau)\mathrm{d}\tau. \tag{7}$$

Combining equation (6) into the left hand side of equation (7) together with equation (4) gives

$$A_i\left(\frac{\omega_i - \omega_{i0}}{\alpha}\right) \propto \int A_s(\tau + \Delta t) A_p^2(\tau)\mathrm{d}\tau, \tag{8}$$

where ω_{i0} is the central frequency of the idler wave and $A_i(\omega_i)$ is the spectrum of the idler wave. Thus, the cross-correlation of the signal wave with the pump wave is proportional to the scaled spectrum of the idler wave. Therefore, by correctly chirping the pump and the signal waves and utilizing the PMD, the spectrum of the resulting idler wave is proportional to the cross-correlation between the signal wave and the square of the pump wave.

The accuracy and resolution of the resulting cross-correlation depends on the bandwidth of the idler beam. If the idler beam is broad-band then intensities from adjacent Δt will mix and the cross-correlation would not be resolved. The bandwidth of the idler beam depends on the chirping and on the FWM process time-scale. Long chirping narrows the bandwidth and increases the resolution; however, it also lowers the instantaneous power which reduces the FWM efficiency. Thus, there is a tradeoff between resolution and sensitivity.

3. Experimental results of the optical cross-correlator

To verify the basic concept of our approach, we demonstrate that the generated idler from appropriately chirped broadband signal and pump waves is narrow-band and its frequency is a function of the time delay between the pump and the signal. The experimental configuration for measuring the spectrum of the idler generated from the chirped pump and signal is presented in figure 1. An ultra-short pulse is stretched in time with a 110 m length of single-mode fiber (SMF) such that it is chirped by 1.95 ps nm^{-1}. The pulse is then split into two separate arms that contain bandpass filters to produce a signal at 1573.5 ± 6 nm and a pump at 1561 ± 4 nm with peak power of about 100 mW for both waves. The pump is stretched in time using another 110 m of SMF to 3.95 ps nm^{-1}. Using a tunable narrow band filter followed by a fast (30 GHz) photo-detector connected to a sampling scope, we measured the exact arrival time for each wavelength to obtain a spectrogram of both the pump and the signal waves, figure 1(a).

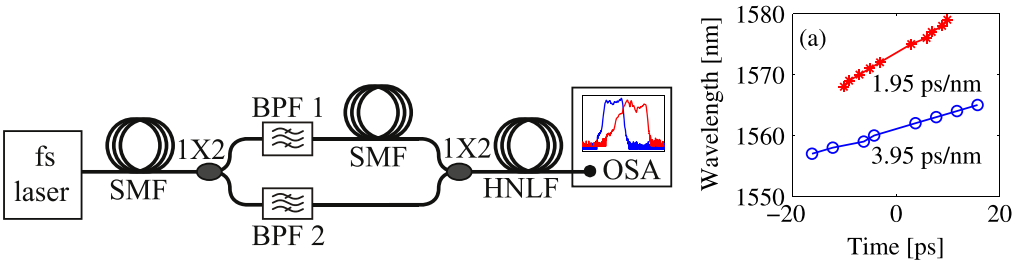

Figure 1. Left: schematic of the experimental configuration for measuring the idler generated by the chirped signal and pump. HNLF—highly nonlinear fiber; 1X2—50/50 beam splitter; OSA—optical spectrum analyzer; SMF —110 m of single mode fiber; BPF—band-pass filter, where the center wavelength of BPF 1 is 1561 ± 4 nm, and BPF 2 is 1573.5 ± 6 nm.[3] Right: measurements of the wavelength as a function of time for the pump (circles) and the signal (asterisks).

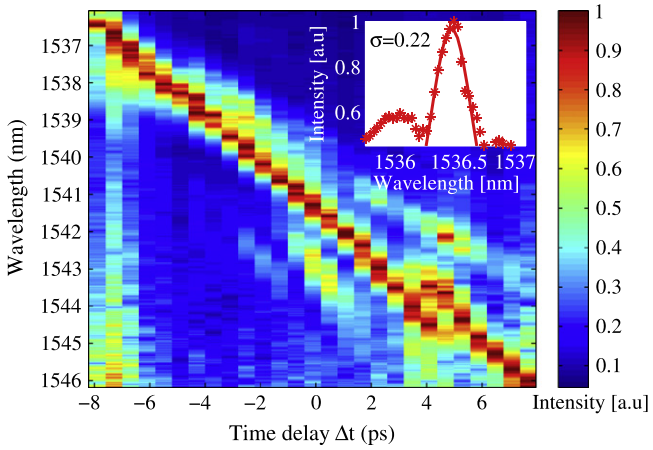

Figure 2. Spectra of the idler for different time delays between the pump and the signal. Inset—typical spectrum at a specific time delay with a Gaussian fit. The width of the gaussian fit is 0.22 nm.

We inject both waves into a short section of highly nonlinear fiber (HNLF) (CorActive SCF-UN-3/125-25) and measure the spectrum of the resulting idler wave as the time delay between the pump and the signal waves is varied. The spectra are shown in figure 2, where red denotes high intensity and blue denotes low intensity. The inset shows a single spectrum at a specific time delay, and its calculated width is 0.22 nm. Here we use 2 m of HNLF, which in terms of nonlinearity is equivalent to a 0.3 mm long silicon waveguide, the idler is clearly detected for all time delays (from −8.5 ps to 8.5 ps), and the width of the peak is less than 0.25 nm. We attribute the noise at the long wavelength region to be due to self phase modulations of the pump wave. This noise can be reduced by using signal and pump waves that have a greater separation in the spectral domain.

Next, we present that the cross-correlation between two arbitrary input functions can be determined by measuring the spectrum of the generated idler wave. The input functions are encoded on both the signal and the pump waves using fiber Bragg gratings that are serially connected. In order to account for the square of the pump in equation (1), we encode on the pump the square root of the input data. In principle, one could use a diffraction grating followed by a spatial light modulator or a nonlinear process to encode the input function in real-time. The experimental configuration is presented in figure 3. Here the signal and the pump waves are orthogonally polarized, and the HNLF is replaced with a silicon nanowaveguide with high birefringent. The waveguide is 1 cm long and has a rectangular cross-section of 710 × 310 nm with a PMD of 18 ps cm^{-1}. After encoding the input functions, the pump and the signal waves are combined by a polarization beam combiner and injected into the silicon nanowaveguide. The signal is injected 9 ps before the pump, as shown in figure 3(a). Due to the PMD of the silicon nanowaveguide, the signal wave propagates slower than the pump wave such that it passes through the pump within the waveguide and exits 9 ps after the pump wave, figure 3(b). We filter the idler from the output channel of the nanowaveguide with a band-pass filter followed by a polarization beam splitter and measure the idler spectrum. The normalized idler spectrum is presented in figure 4 (dotted curve) together with the calculated cross-correlation between the signal and pump waves (solid curve).

In our case, the losses where 10 dB cm^{-1}, which limit the length of the waveguide to no more than few centimeters, the input and output losses to the silicon waveguide were 5 dB, and the coupling efficiency into the optical spectrum analyzer was higher than 0.6. The idler wave power was 10 μW due to the low FWM efficiency. By designing a waveguide with lower losses it will be possible to increase the efficiency and the length of the optical cross-correlator. Also, our current design is sensitive to mechanical noises mainly due to the fiber-lenses which couple light between fibers and the silicon waveguide. Therefore, it is preferable to switch to highly nonlinear polarization maintaining fibers, or tightly coiled Chalcogenide glass fibers which have the same nonlinearity as silicon waveguide with lower losses and higher PMD.

4. Experimental demonstration of pattern recognition with optical cross-correlator

Finally, we demonstrate a proof-of-principle concept were this system is able to distinguish between two distinct input signals. Each signal is produced using serially-connected fiber Bragg gratings that reflects different wavelength channels from a pulse with a Gaussian shaped spectrum. The resulting

[3] These are only schematics of the experimental configuration symplified for the reader. The experimental setup was fully integrated inside waveguides.

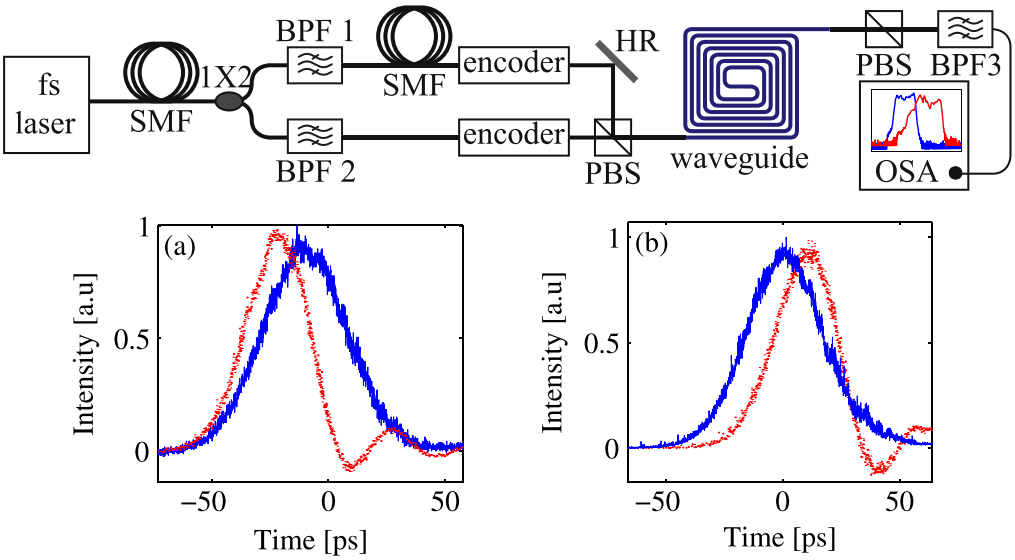

Figure 3. Top: schematic of the experimental configuration for the optical cross-correlator in the silicon nanowaveguide. PBS—polarization beam splitter; 1X2—50/50 beam splitter; HR—high reflection mirror; OSA—optical spectrum analyzer; SMF—110 m of single mode fiber; BPF—band-pass filter, where the center wavelength of BPS 1 is 1561 ± 4 nm, BPS 2 is 1573.5 ± 6 nm, and PMS 3 is 1545 ± 10 nm (see footnote 3). (a) temporal measurements of the pump wave (solid curve) and the signal wave (dashed curve) before the waveguide; (b) temporal measurements of the pump wave (solid curve) and the signal wave (dashed curve) after the waveguide.

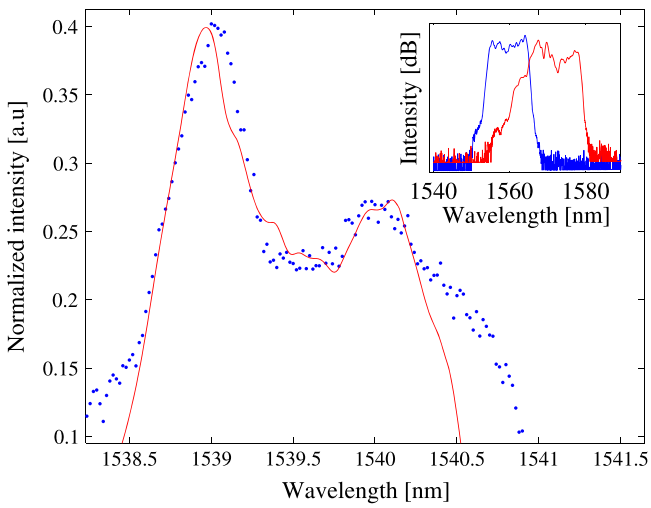

Figure 4. Normalized experimental results of the idler spectrum (dots) together with the calculated cross-correlation of the pump with the signal. Inset shows the spectrum of the pump wave (dashed curve) and the spectrum of the signal (solid curve).

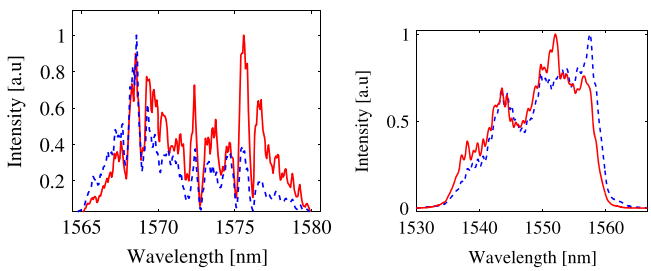

Figure 5. Left: measured spectra of the two signals. Right: calculated idler spectrum by cross-correlation of the two signals with the pump. Dashed curve: signal *a*, solid curve: signal *b*.

spectra are presented in figure 5 (left) where the dashed curve denotes signal *a*, and the solid curve denotes signal *b*. We code '0110111010' into signal *a* and '1111010111' into signal *b*. The temporal length of both signals is less than 4 ps which is equivalent to transfer bit-rate higher than 1 THz, therefore, no electronic detector can distinguished between these two signals. We tailor the spectrum of a pump wave such that cross-correlation of signals *a* and *b* with the same pump wave results in different idler waves, so the two signals can be distinguished using our optical cross-correlator. The calculated cross-correlation of the pump wave with each signal waves is presented in figure 5 (right) where the dashed curve denotes the cross-correlation with signal *a* and the solid curve with signal *b*. The peak in the calculated cross-correlation of *a* is displaced compared to the cross-correlation of *b* by 5.5 nm.

We acquire the spectra of the two idler waves resulting from the FWM interaction between the pump wave and signals *a* and *b*, and the results are presented in figure 6. As evident, the peak of spectrum *a* (dashed curve) is at 1553.7 nm and the peak of spectrum *b* (solid curve) is at 1548 nm. Decoding of the output is done by measuring the wavelength of the peak intensity in the idler spectrum. The peaks in the spectra are displaced by 5.7 nm which is close to the calculated result of 5.5 nm. We attribute the discrepancy between the calculated idler spectrum shift and the measured idler spectrum to inaccuracies in realigning the system after switching from signal *a* to signal *b* since they are produced in different optical arms. We also obtained some measurement artifact and noise due to the low efficiency of the FWM process. Nevertheless, our system readily distinguishes between these two signals with a signal to noise ratio of about 4. Switching to polarization maintaining nonlinear fiber will increase the efficiency and the signal to noise ratio.

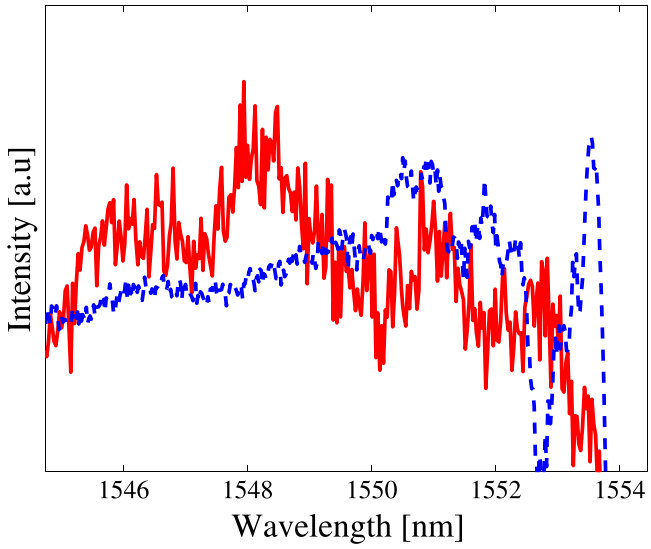

Figure 6. Measured spectra of the two idler waves created through four wave mixing of the pump with signal waves *a* (dashed curve) and *b* (solid curve).

5. Conclusions

In summary, we demonstrated a system for measuring single-shot optical cross-correlation between two signals using a nanowaveguide. This was done by measuring the spectrum of the idler wave generated from FWM process between the pump and the signal waves. We demonstrated a cross-correlation of an input pulse and how this device can distinguish between two inputs. This demonstration is an important step toward a full optical routers and integrated optical processing devices. This device can be implemented in optical routers for header detection, as a trigger mechanism for ultra-fast cameras and in ultrafast pulse characterization schemes. The accuracy by which the cross-correlation is measured can be improved by designing a suitable waveguide with high PMD concordantly with low losses.

References

[1] OMahony M J, Simeonidou D, Hunter D K and Tzanakaki A 2001 The application of optical packet switching in future communication networks *IEEE Commun. Mag.* **39** 128–35

[2] Hauer M C *et al* 2002 Dynamically reconfigurable all-optical correlators to support ultra-fast internet routing *Optical Fiber Communication Conf. Exhibit* pp 268–70

[3] Goda K, Tsia K K and Jalali B 2009 Serial time-encoded amplified imaging for real-time observation of fast dynamic phenomena *Nature* **458** 1145–9

[4] Kim S H, Goda K, Fard A and Jalali B 2011 Optical time-domain analog pattern correlator for high-speed real-time image recognition *Opt. Lett.* **36** 220–2

[5] Trebino R 2002 *Frequency-Resolved Optical Grating: The Measurement of Ultrashort Laser Pulses* (Berlin: Springer)

[6] Trebino R and Kane D J 1993 Using phase retrieval to measure the intensity and phase of ultrashort pulses: frequency-resolved optical gating *J. Opt. Soc. Am.* A **10** 1101

[7] Casasent D and Psaltis D 1976 Position, rotation, and scale invariant optical correlation *Appl. Opt.* **15** 1795

[8] Sun C-C, Lee T-X, Ma S-H, Lee Y-L and Huang S-M 2006 Precise optical modeling for LED lighting verified by cross correlation in the midfield region *Opt. Lett.* **31** 2193

[9] Gyuzalian R N, Sogomonian S B and Horvath Z Gy 1979 Background-free measurement of time behaviour of an individual picosecond laser pulse *Opt. Commun.* **29** 239–42

[10] Beye M *et al* 2012 X-ray pulse preserving single-shot optical cross-correlation method for improved experimental temporal resolution *Appl. Phys. Lett.* **100** 121108

[11] Iaconis C and Walmsley I A 1998 Spectral phase interferometryfor direct electric-field reconstructionof ultrashort optical pulses *Opt. Lett.* **23** 792

[12] Linden S, Giessen H and Kuhl J 1998 XFROG—A new method for amplitude and phase characterization of weak ultrashort pulses *Phys. Status Solidi* B **206** 119–24

[13] Zhang J Y, Lee C K, Huang J Y and Pan C L 2004 Sub femto-joule sensitive single-shot OPA-XFROG and its application in study of white-light supercontinuum generation *Opt. Express* **12** 574

[14] Eng J K, Fischer B, Grossmann J and MacCoss M J 2008 A fast SEQUEST cross correlation algorithm *J. Proteome Res.* **7** 4598–602

[15] Ophir N, Lau R K W, Menard M, Salem R, Padmaraju K, Okawachi Y, Lipson M, Gaeta A L and Bergman K 2012 First demonstration of a 10 Gb s^{-1} end-to-end link at 1884 nm based on four-wave mixing of telecom-band RZ data in silicon waveguides *Photonics Technol. Lett.* **24** 276–8

[16] Lee B G, Biberman A, Turner-Foster A C, Foster M A, Lipson M, Gaeta A L and Bergman K 2009 Demonstration of broadband wavelength conversion at 40 Gb s^{-1} in silicon waveguides, Photon *Photonics Technol. Lett.* **21** 182–4